

TWO-DIMENSIONAL REACTION OF BIOLOGICAL MOLECULES STUDIED BY WEIGHTED-ENSEMBLE BROWNIAN DYNAMICS

I.A. SHKEL

*Dept. of Biochemistry, Univ. of Wisconsin-Madison, 433 Babcock Drive,
Madison, WI 53706-1544, USA*

S. KIM^a

*Dept. of Chemical Engineering, Univ. of Wisconsin-Madison,
1415 Engineering Drive, Madison, WI 53706-1691, USA*

Computer simulations offer critical insights into the reaction of biological macromolecules, especially when the molecular shapes are too complex to be amenable to analytical solution. In this work, the Weighted-Ensemble Brownian (WEB) Dynamics simulation algorithm is adapted to a reaction of two unlike biological molecules, with the interaction modeled by a two-parameter system: a spherical molecular depositing on a target region of an infinite cylinder with a periodic boundary conditions. The original algorithm of Huber and Kim¹ is streamlined for this class of reactive models. The reaction rate constant is calculated as a function of relative sizes of the reactive to non-reactive regions of the cylindrical molecule. An analytical expression for the rate constant is also obtained from the solution of the diffusion equation for the special case of a constant-flux boundary condition. Good agreement between analytical and simulation results validates the applicability of WEB Dynamics to a reaction of molecules of complicated shape. On the other hand, the simple form of our analytical expression is useful as a testing case for other simulation and numerical techniques.

1 Introduction

Biological molecules react only when they are in particular orientations because of the presence of reactive sites. Consequently, the geometry of a reactive site is of paramount importance to drug design. But because of the complicated shapes of many biological molecules, an analytical treatment of their relative motion is difficult; thus computer simulation techniques, such as Brownian Dynamics^{2,3}, are widely used for this purpose. Although molecular dynamics simulations are commonly applied to detailed molecular models, Brownian dynamics allow access to longer time scales, albeit with the loss of molecular resolution of the solvent molecules. Brownian dynamics is often employed in conjunction with molecules modeled as combinations of solid bodies of relatively simple shapes: spheres^{3,4}, spheroids⁵, cylinders⁶, with

^aPresent address: Parke-Davis Pharmaceutical Research, 2800 Plymouth Road, Ann Arbor, MI 48105, USA

reactive sites described by local charge distributions or surface reactivity^{4,7}. For protein-protein reactions, such models have been widely investigated by Brownian Dynamics simulations^{7,8,9} as well as analytically^{10,11,12,13}, with the protein shapes modeled as spheres. Wu *et al.*¹⁰ give an extensive review of these and other related works. Of special note is the analytical approach by Shoup *et al.*¹¹ where diffusion of one spherical molecule on another is considered in the constant flux approximation with the boundary condition for probability on the reactive site ($P = 0$) replaced by a constant probability flux ($\partial P/\partial n = \text{const}$). This method, although approximate, gives an expression for the rate constant in a closed analytical form that offers useful insights.

The prior works mentioned above were directed generally toward models of protein-protein interaction. However for the reaction of a small molecule with DNA or RNA a modified approach is necessary due to disparate length scales of the reacting species. In this study, one molecule is presented as a sphere, another as a three-segment cylinder with one segment highly reactive to the first molecule. We applied the Weighted-Ensemble Brownian (WEB) Dynamics for our Brownian dynamics implementation because of its demonstrated efficiency in simulation of complex geometries^{1,5}. WEB Dynamics achieves such acceleration by dividing the configuration space into bins in a manner that facilitates biased sampling of specific regions of the configurations of greatest interest (e.g. the reactive configuration). In one-dimensional problems, the bin generation algorithm is obvious¹; for two-dimensional problems, the generation of bins becomes non-trivial. We suggest various criteria (shape of bin boundaries, bin thickness and a size of the time step in each bin) for setting up bins for multi-dimensional cases, which take into account the expected shape of the probability density and flux. Our bin algorithm yields fast convergence of the results, and the resulting WEB Dynamics algorithm thus becomes a convenient tool to investigate this class of biomolecular reactions. Simulations were performed in a wide range of relative sizes of the cylinder reactive surface including the limiting case of the completely reactive cylinder.

We also present an approximate solution of the cylindrical diffusion equation by the method similar to the method used by Shoup *et al.*¹¹ (their analysis was for a spherical geometry). We substitute the boundary condition of zero probability on the reactive surface of the cylinder ($P = 0$) by the boundary condition of constant and specified flux ($\partial P/\partial n = \text{const}$), subject to a requirement to minimize discrepancy from the exact solution. We obtained a simple analytical expression for the rate constant as a function of parameters (sizes of molecules, reactive segment etc.). Both analytical and simulation results are in good agreement over the full range of these parameters.

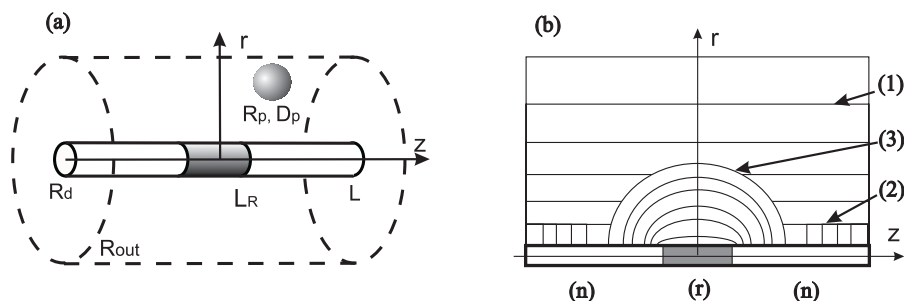


Figure 1: Molecular model (a) and bin system (b). The sphere molecule has radius R_p and diffusion coefficient D_p . The cylindrical molecule has radius R_d , reactive segment (r) of length $2L_R$, and two non-reactive segments (n). The simulation region is the cylinder of radius R_{out} and length $2L$ co-axial with the molecule. The axis z is the cylinder axis, $z = 0$ is the center of the reactive segment. Bin system (b) consists of 100 bins: 25 cylindrical bins (1), 25 cylindrical bins (2), and 50 ellipsoidal bins (3).

2 Model of Molecules

We consider a reaction of two species, A and B, $A + B \rightarrow AB$, with corresponding concentrations n_A and n_B . The reaction rate constant, k , is defined by the equation

$$\frac{dn_A}{dt} = k n_A n_B. \quad (1)$$

There are two ways to calculate the rate constant of the reaction: through the flux of probability density, obtained from a solution of the diffusion equation, or through the flux of particles on the reactive surface, which can be obtained from a computer simulation based on the corresponding stochastic differential equation. We will examine both approaches.

To make our analytical analysis and computer simulation effective we need a simplified model of the reactive molecules. Figure 1(a) shows the molecular model. The first molecule is modeled as a sphere of radius R_p . The sphere is subjected to Brownian motion with the translational diffusion coefficient D_p . For the present study, we consider the whole surface of the sphere to be reactive to the second molecule, but this is not an inherent limitation of the method. The second molecule is a long cylinder of radius R_d . The part of the cylinder of length $2L_R$ is highly reactive to the first molecule. In order to model molecules with multiple reactive sites, we assume that there are several reactive segments on the cylinder separated by non-reactive segments. For simulation and analytical treatment, a cylinder fragment of length $2L$ is placed inside of the simulation region, the co-axial cylinder with the same length $2L$ and radius R_{out} . The reactive part of the cylinder fragment is placed in the center of the

simulation region. Total length of the fragment, $2L$, represents an average length per reactive site of the cylindrical molecule, while $2L_R$ is a typical size of such site. The radius of the simulation region, R_{out} , is chosen through the condition that the volume of the simulation region is the volume per length $2L$ of the first molecule and related to its concentration in the solution. The diffusion of the cylinder is neglected because of much higher size of cylindrical molecule compare to the sphere. We also assume that the bulk concentration of the first molecule is known and use it as a boundary condition on the outer surface of the simulation region. In the cylindrical coordinate system (Fig. 1), r is the radial coordinate, z is the coordinate along the cylinders with $z = 0$ corresponding to the center of the reactive segment.

With all these assumptions, the problem reduces to a diffusion of a point particle with the translational diffusion coefficient D_p to a cylinder of radius $R_D = R_d + R_p$ and non-uniform reactive surface. Although the particle moves in three dimensional space, the problem has a two-dimensional character since all values of interest (probability density, probability flux) depend only on two spatial coordinates, r and z . The dependence on the z -coordinate arises due to the presence of reactive site on the cylindrical molecule. Finally, we note that the particle is not to be confused with the molecular species - the particle represents the coordinates of the reacting sphere in the configuration space.

3 Simulations

3.1 WEB Dynamics Algorithm

In this section we briefly outline the WEB Dynamics algorithm as it is described by Huber *et al.*¹ A simulation region is a cylinder of length $2L$, inner radius R_D , and outer radius R_{out} . Many particles move inside the simulation region independently. Particles start from some initial configuration (it may be random uniform placement of particles or anything else), and move according to Brownian Dynamics equation²

$$\mathbf{X}_{i+1} = \mathbf{X}_i + \mathbf{W}_i \sqrt{2 D_p \Delta t} - \mathbf{F} D_p \Delta t / k_B T. \quad (2)$$

Here \mathbf{X}_i are Cartesian coordinates of the particle on the i -th time step, Δt is the time step size, \mathbf{W}_i is the vector of the Gaussian random values with zero mean and unit variance, \mathbf{F} is the systematic force acting on a particle, k_B is the Boltzmann constant, and T is the temperature. On the reactive part of the cylinder, the instantaneous reaction takes place (zero probability to find a particle). A particle is terminated each time it reaches the reactive segment, and reintroduced on the outer surface of the simulation region to preserve the

steady state condition. Conditions on the non-reactive part of the cylinder and at $z = \pm L$ are reflective conditions (zero particulate flux). If during the time step a particle penetrates one of these surfaces, change of the coordinate along the surface is accepted, but other coordinates are kept as before the time step. If a particle goes out of the simulation region at the outer surface ($r = R_{out}$), the step is not accepted.

The simulation region is divided into the bins (layers), as will be discussed in detail in the next section. On the first time step equal weights are assigned to all particles. At the end of each time step the weights of particles are recalculated by combining and dividing particles to have the same number of particles in each bin. These “weighted particles” represent probability packets rather than real molecules, because their weight is equal to an average probability to find real particle in this part of the configuration space

$$W_i \approx \langle P_i \rangle dV_i. \quad (3)$$

Here W_i is total weight of the particles in the i -th bin, $\langle P_i \rangle$ is the average probability density in the bin and dV_i is the volume of the bin. The Dirichlet boundary condition (probability density specified at boundary) at the outer surface would be satisfied if the weight of particles in the closest to the outer surface bin is equal to the volume of this bin.

The weight of particles arriving on the reactive segment was accumulated over some number of time steps N_f , and the particle flux was calculated as the accumulated weight per unit time $J_W = \sum_j W_j / (N_f \cdot \Delta t)$. The number of time steps for accumulating the flux was chosen according to the condition $N_f \cdot \Delta t = 0.1 \cdot T_c$, where $T_c = R_D^2 / D_p$ is the characteristic time for the problem. The rate constant is connected with the accumulated flux through the volume of the simulation region, V , and Avogadro’s number, N_A .

$$k = J_W V N_A. \quad (4)$$

Time of calculation in WEB Dynamics is proportional to the number of bins and to the number of particles per bin. We used 100 bins and 4 particles per bin in all simulations.

3.2 Criteria for Creating Bin Structure

There are two important issues, which have to be taken into account in dividing a simulation region into bins. The first one is connected with Eq.3 stating that the weight of particles in each bin is the average probability in this bin. The boundaries of the bins are chosen to follow the expected “contour lines” of probability, so that averaging during simulation does not give a round-off

error due to combining of particles with very different weights. Another issue is equilibrating of the system. Since particles in the simulation start from some initial configuration, it takes some time for distribution of “weight” to reach steady state. Thus, a part of simulation time always has to be spent on equilibrating of the particle weight distribution. It is essential to choose appropriate bin system in order to reduce this time. For one-dimensional case¹, the choice of the bin system is obvious, bins are layers, whose long boundaries are the constant coordinate surfaces. In such configuration, the probability flux is normal to the bin boundaries, and that ensures fast interchange of particles between neighbor bins and uniform probability in each bin.

For multi-dimensional case, we also choose bins as layers of some shape and require two criteria to be satisfied: boundaries between bins should be perpendicular to the principal directions of the probability flux, and the bin thickness should be comparable to the average displacement of the particles during one time step. Due to the first condition, there is no significant probability gradient along the bin boundary, and probability rather uniform inside the bin. Furthermore, motion of the particle in each bin is much more favorable across the bin than along its boundary, and particles have sufficient chance to move to the next bin during one time step.

There are three major directions of the flux in the considered problem: in r -direction toward the cylinder, toward the reactive segment and along the cylinder. Each direction prevails in some particular region of the space. In accordance with these three directions, the bin structure consists of three regions (Fig. 1(b)): 25 cylindrical bins in r -direction far from the cylinder surface; 25 cylindrical bins in z -direction along the non-reactive part of the cylinder surface, and 50 ellipsoidal bins around the reactive segment. Ellipsoidal bins were constructed by creating ellipses with end points of the reactive segment as focuses and rotating them around z -axis. According to criteria above, thickness of a bin, ΔX_{bin} , should be of order of an average random displacement of the particle in this bin, $\Delta X_B = \sqrt{2 D_p \Delta t}$.

$$\Delta X_{bin} < \Delta X_B. \quad (5)$$

Variation of the time step also accelerates the calculations¹. We scale the time steps in each bin using the condition that the random displacement of a particle, ΔX_B , is bigger than the systematic displacement, $\Delta X_F = F D_p \Delta t / k_B T$. The resulting time step in each bin satisfies:

$$\Delta t \ll 2 D_p^{-1} (k_B T / F)^2. \quad (6)$$

Thus, in the presence of a force, the value of the force influences the time step in each bin and the bin thickness. In the case of pure diffusion ($F = 0$),

the minimum time step, in the bins close to the reactive segment, was chosen $\Delta t_{min} = 10^{-4} T_c$, and the maximum time step, in the bins close to the outer surface, $\Delta t_{max} = 100 \Delta t_{min}$.

If all conditions above are satisfied, simulations reach steady state on the time of T_c . Total simulation time was $10 T_c$ in order to reduce statistical uncertainty of the results.

4 Analytical Solution of Diffusion Equation

4.1 Cylindrical Diffusion Equation

To describe the reaction of two molecules we employ the steady-state diffusion equation for probability density $P(r, z)$ of the sphere molecule within the simulation region. For the model considered here there are periodical reactive segments on the cylinder. Because of this, the probability flux on the ends of the cylindrical molecule is zero: the sphere has the equal probabilities to go to either reactive segment ($\partial P / \partial z = 0$). There is no reaction on the non-reactive part of the cylinder surface, and flux here is also zero ($\partial P / \partial r = 0$). The probability to find the sphere on the reactive part of the cylinder is zero due to instantaneous reaction ($P = 0$). The probability density on the outer surface is the known value, which could be set to 1 to simplify algebraic manipulations.

Using L as a characteristic length, we can write the diffusion equation and boundary conditions in the dimensionless form.

$$\frac{1}{r^*} \frac{\partial}{\partial r^*} \left(r^* \frac{\partial P}{\partial r^*} \right) + \frac{\partial^2 P}{\partial z^{*2}} = 0, \quad (7)$$

$$(\partial P / \partial z^*)|_{z^* = \pm 1} = 0, \quad (\partial P / \partial r^*)|_{r^* = R_D^*, L_R^* < |z^*| < 1} = 0, \quad (8)$$

$$P|_{r^* = R_D^*, |z^*| < L_R^*} = 0, \quad P|_{r^* = R_{out}^*} = 1. \quad (9)$$

where values, denoted by the star, are reduced values $(var)^* = (var)/L$, and $(var) = \{r, z, L_R, R_D, R_{out}\}$. The flux J_R of probability density on the reactive part of the surface S_R of one molecule of species B is connected with the rate constant through the Avogadro number N_A ,

$$k = J_R N_A, \quad J_R = - \int_{S_R} D_p \frac{\partial P}{\partial x_i} n_i dS = -D_p L \int_{S_R^*} \frac{\partial P}{\partial x_i^*} n_i dS^*. \quad (10)$$

For the uniformly reactive cylinder the term $\partial^2 P / \partial z^{*2}$ in Eq.7 is absent; the solution of the equation follows upon performing the integration and yields the expression for the rate constant:

$$k_{(L_R=L)} = 4\pi L D_p N_A (\ln(R_{out}/R_D))^{-1}. \quad (11)$$

The following section will consider a solution of the diffusion equation for the less trivial case of a non-uniform reactive surface of the cylinder.

4.2 Non-uniformly Reactive Cylinder

The problem, as formulated in the previous section, is challenging due to the mixed boundary conditions: the probability is specified on one part of the surface and the flux is known on the rest of the surface. It is important to recognize that we are not interested in the details of the probability distribution in the space, but only in the flux on the reactive segment. Thus, we can substitute this problem by a problem with another, more convenient, boundary condition, which gives the same flux on the reactive segment. Instead of zero probability of the sphere to be found on the surface of the reactive segment, we will stipulate a constant probability flux J_0 on this part of the surface. The value of the constant, J_0 , is determined from the additional condition that average probability density at the reactive segment is zero

$$\left. \frac{\partial P}{\partial r^*} \right|_{r^*=R_D^*, 0 < |z^*| < L_R^*} = J_0, \quad \int_{-L_R^*}^{L_R^*} P(r^*, z^*) dz^* = 0. \quad (12)$$

The eigenfunction expansion for the present problem is a Fourier-Bessel series of the form:

$$P = c \ln(r^*/a) + \sum_{n=1}^{n=\infty} [A_n K_0(ir^*) + B_n I_0(ir^*)] \cos(iz^*). \quad (13)$$

Here K_j and I_j are the Bessel functions of order j , $i = \pi n$, n is a positive integer number, a , c , A_n and B_n are constants. After determining these constants from the boundary conditions Eq. 8, 9 and the value of the constant J_0 from the Eq. 12, we have following expression for the rate constant ($k = N_A J_R = N_A D_p L J_0 S_R^* = 4\pi N_A D_p L J_0 L_R^* R_D^*$)

$$k = 4\pi D_p N_A L (\ln(R_{out}/R_D) + S)^{-1}, \quad (14)$$

$$S = \sum_{i/\pi=1}^{i/\pi=\infty} \frac{2 \sin^2(iL_R^*) (K_0(iR_D^*) I_0(iR_{out}^*) - I_0(iR_D^*) K_0(iR_{out}^*))}{(iL_R^*)^2 iR_D^* (K_1(iR_D^*) I_0(iR_{out}^*) - I_1(iR_D^*) K_0(iR_{out}^*))}. \quad (15)$$

To calculate the rate constant from this expression, we need to know the sum S . Obviously, in the limit of uniform reactive surface ($L_R^* \rightarrow 1$), S is zero, and the expression for the rate constant Eq. 14 reduces to Eq. 11 for uniformly reactive cylinder. The function $G(x)$ is always less than 1, and goes to 1 as

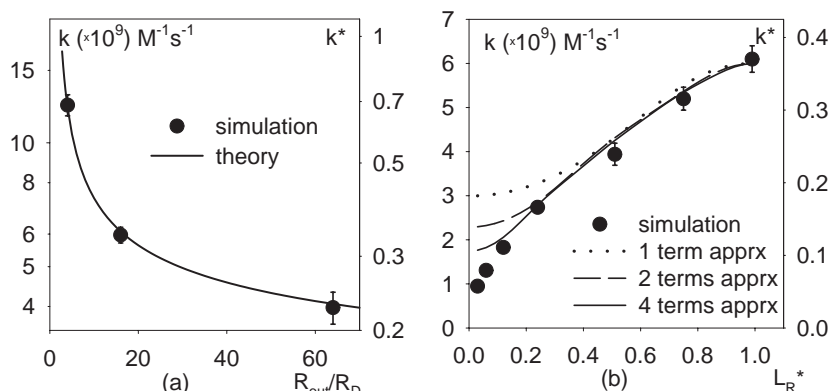


Figure 2: Rate constant for uniformly (a) and partly (b) reactive cylinder. The right axis on each graph is the reduced rate constant $k^* = k/4\pi D_p N_A L$, the left axis is the actual value of k for $L = 400 \text{ \AA}$ and $D_p = 5.6 \cdot 10^{-3} \text{ \AA}^2/ps$. Reduced cylinder radius for all simulations is $R_D^* = 0.125$. The rate constant for uniformly reactive cylinder (a) is plotted as a function of the simulation region size R_{out}/R_D . Simulation results (dots) are for three values of the ratio $R_{out}/R_D = 4, 16, 64$. The rate constant of the partly reactive cylinder (b) is plotted as a function of the relative size of the reactive segment L_R^* for the ratio $R_{out}/R_D = 16$. Simulation results (dots) are for $L_R^* = 0.025; 0.05; 0.125; 0.25; 0.5; 0.75; 1$. Lines represent calculations by analytical formula with the sum S truncated up to several terms.

$x \rightarrow \infty$. For some range of L_R^* , the first term alone in the sum S may be accurate enough for most applications. At moderate values of L_R^* , $0.4 < L_R^*$, the difference caused by sum truncation is of the order of several percent. In this range, we can further simplify expression for the rate constant replacing S by the first term. Smaller values of L_R^* require more terms in the sum S in order to obtain an accurate result. At $L_R^* = 0.25$, first two terms in the sum S give result with accuracy of 3 percent, while for $L_R^* = 0.05$, 6-8 terms are necessary for the same accuracy.

5 Simulation Results

Since simulation were performed using reduced values of geometrical parameters L_R^* , R_D^* , R_{out}^* , the resulting rate constant is also a reduced quantity according to the formula $k^* = k/(4\pi N_A D_p L)$. We present simulation results (Fig. 2) in two forms, the right axis is the reduced values of the rate constant k^* , and the left axis is the actual values of k calculated for $L = 400 \text{ \AA}$ and $D_p = 5.3 \cdot 10^{-3} \text{ \AA}^2/ps$, which is the diffusion coefficient of a sphere of radius $R_p = 37.5 \text{ \AA}$ in water at room temperature. For all simulations the value $R_D^* = 0.125$ is used, while values of L_R^* and R_{out}^* were varied.

First of all, we compared simulation results for uniformly reactive cylinder to the exact analytical solution Eq. 11 (Fig. 2(a)). All 100 bins in this one-dimensional case were cylindrical bins such as (1) on Fig. 1(b). Figure 2(a) represents the rate constant of uniformly reactive cylinder as a function of outer radius, circles are the simulation results, uncertainties are shown as vertical bar (one standard deviation), and the solid line is the analytical result. Simulations were performed for three values of outer radius, $R_{out}/R_D = 4, 16, 64$. The ratio R_{out}/R_D is connected with concentration of cylindrical molecule through the requirement that the volume of the simulation region is the volume per length $2L$ of the cylindrical molecule. For the cylinder molecules of total length 8000 \AA (10 fragments), we used values of the ratio R_{out}/R_D corresponding to concentrations $3 \cdot 10^{-6} \text{ M}$, $2 \cdot 10^{-7} \text{ M}$, and $1.2 \cdot 10^{-8} \text{ M}$.

In addition, simulations were performed for various sizes of the reactive segment. Figure 2(b) represents the rate constant as a function of the relative size L_R^* of the reactive segment. Circles are the simulation results and the lines are the values, calculated from Eq. 14 with the sum S written to just a few terms. It is clear, that even the first term alone in the sum S of Eq. 14 gives a good approximation for moderate values of the reactive segment (the relative size of the reactive segment L_R^* is bigger then 0.4). Taking into account three more terms allows extension of the application of the Eq. 14 down to $L_R^* = 0.125$.

6 Discussion

The work of Huber and Kim¹ has been extended to bin generation in a two-dimensional space. Good agreement between simulation and analytical results validates the application of the WEB Dynamics algorithm to two-dimensional space. (Simulations with alternative bin systems yielded correct results but with a higher level of statistical noise and long equilibration time.) The approach suggested here can be extended to cases with more than two dimensions (e.g., arising from the parametrization of the shapes/states of a reactive site, the rotational diffusion of the molecules, and the presence of reactive sites on both reacting molecules).

In modeling of a reactive site of arbitrary shape, fluxes in two principal directions have to be taken into account: normal to the surface due to difference in probabilities between the reactive site and distant part of space; tangential flux due to the difference in probabilities on the reactive and non-reactive parts of the surface. Therefore, close to a reactive site, bins should be organized so that they are parallel to the surface; and close to a non-reactive surface, bin boundaries should be perpendicular to the surface to insure tangential flux.

Incorporation of rotational degrees of freedom dramatically increases the simulation time in traditional Brownian Dynamics because particles now have to explore configuration states in many more dimensions. Spatial proximity to a reactive site is insufficient; the correct orientation is also required. The essence of WEB Dynamics, combining of uninteresting states, overcomes this problem. An efficient bin structure could be built in the cases when the rotational diffusion is significant, provided that we take into account not only spatial coordinates but orientation angles as well.

Moreover, we expect that the CPU time for a non-uniformly reactive case will be essentially the same as for the corresponding uniformly reactive case. We observed this in our simple example, when simulations in one-dimensional space (uniformly reactive cylinder) and in two-dimensional space (partly reactive cylinder) show the same times of equilibration, both on the order of characteristic time T_c and only a function of geometrical parameters and diffusion coefficients. Huber *et al.*¹ compared the calculation time for one-dimensional space by WEB Dynamics and traditional Brownian Dynamics, and showed that WEB Dynamics is 14,000 times faster. For a multi-dimensional configuration space this difference in calculation times increases even further.

The computational demands for the present study were as follows. The typical time for a simulation (total simulation time $10 T_c$) on a Pentium II 266 MHz PC is 1.5 hours. Even quicker *estimates* of the rate constant could be obtained in 10-15 minutes by performing simulations of duration T_c . Clearly, WEB Dynamics can be viewed as a desk-top tool for investigation of simple to complex models of biomolecular reactions.

The considered case of pure diffusion gives the reaction rate constant of the order $10^9 - 10^{10} M^{-1} s^{-1}$ for $R_p = 37.5 \text{ \AA}$, $R_d = 12.5 \text{ \AA}$, $L = 400 \text{ \AA}$, and $D_p = 5.3 \cdot 10^{-3} \text{ \AA}^2/ps$. This is in the range of typical values for interaction of DNA and proteins¹⁵. This is an encouraging result. Future directions can focus on the incorporation of more realistic force models.

Acknowledgments

This work was supported in part by ONR Grant N00014-92-J-1564 to SK.

References

1. G. A. Huber and S. Kim, Weighted-ensemble brownian dynamics simulations for protein association reactions, *Biophysical J.* **70**, 97 (1996).
2. D. L. Ermak and J. A. McCammon, Brownian Dynamics with hydrodynamic interactions, *J. Chem. Phys.* **69**, 1352 (1978)

3. S. H. Northrup, S. A. Allison, and J. A. McCammon, Brownian dynamics simulation of diffusion-influenced bimolecular reactions, *J. Chem. Phys.* **80**, 1517 (1984).
4. R. E. Kozack, M. J. d'Mello, and S. Subramaniam, Computer modeling of electrostatic steering and orientational effects in antibody-antigen association, *Biophysical J.* **68**, 807 (1995).
5. A. Rojnuckarin, S. Kim, and S. Subramaniam, Brownian dynamics simulations of protein folding: Access to milliseconds time scale and beyond. *Proc. Natl. Acad. Science.* **95**, 4288 (1998).
6. J. D. Dwyer, and V. A. Bloomfield, Computer simulation of bimolecular rate constants for site-specific protein-DNA interactions, *Biophysical J.* **70**, MP448 (1996).
7. J. S. Gupta, and D. V. Khakhar, Brownian dynamics simulation of diffusion controlled reactions with finite reactivity, *J. Chem. Phys.* **107**, 1915 (1997).
8. B. A. Luty, and J. A. McCammon, H.-X. Zhou, Diffusive reaction rates from Brownian dynamics simulations: Replacing the outer cutoff surface by an analytical treatment, *J. Chem. Phys.* **97**, 5682 (1992).
9. H.-X. Zhou, Brownian dynamics study of the influence of electrostatic interaction and diffusion on protein-protein association kinetics, *Biophysical J.* **64**, 1711 (1993).
10. Y.-T. Wu and J. M. Nitsche, On diffusion-limited site-specific association processes for spherical and nonspherical molecules, *Chemical Engr. Science.* **50**, 1467 (1995).
11. D. Shoup, G. Lipari, and A. Szabo, Diffusion-controlled bimolecular reaction rates. The effect of rotational diffusion and orientation constraints, *Biophysical J.* **36**, 697 (1981).
12. H.-X. Zhou, Enhancement of protein-protein association rate by interaction potential: accuracy of prediction based on local Boltzmann factor, *Biophysical J.* **73**, 2441 (1997).
13. S. D. Traytak, Diffusion-controlled reaction rate to an active-site, *J. Chem. Phys.* **102**, 1 (1995).
14. K. Sharp, R. Fine, K. Schulten, and B. Honig, Brownian Dynamics simulation of diffusion to irregular bodies, *J. Phys. Chem.* **91**, 3624 (1987)
15. R. B. Winter, O. G. Berg, and P. H. von Hippel, Diffusion-driven mechanism of protein translation on nucleic acids. 3. The Escherichia coli lac repressor-operator interaction: Kinetic measurements and conclusions, *Biochemistry* **20**, 6961 (1981).